

Clinical Features of a Retinopathy Associated With a Dominant Allele of the *RGR* Gene

Rola Ba-Abbad,^{1,2} Monique Leys,³ Xinjing Wang,⁴ Christina Chakarova,¹ Naushin Waseem,¹ Keren J. Carss,^{5,6} F. Lucy Raymond,^{6,7} Kinga M. Bujakowska,^{8,9} Eric A. Pierce,^{8,9} Omar A. Mahroo,^{1,2,10} Moin D. Mohamed,¹⁰ Graham E. Holder,^{1,2,11} Marybeth Hummel,¹² Gavin Arno,^{1,2} and Andrew R. Webster^{1,2}

¹UCL Institute of Ophthalmology, London, United Kingdom

²Moorfields Eye Hospital, London, United Kingdom

³WVU Eye Institute, West Virginia University, Morgantown, West Virginia, United States

⁴Genetics Laboratory, Department of Pediatrics, University of Oklahoma Health Sciences Center, Oklahoma City, Oklahoma, United States

⁵Department of Haematology, University of Cambridge, Cambridge, United Kingdom

⁶NIHR BioResource-Rare Diseases, University of Cambridge, Cambridge, United Kingdom

⁷Department of Medical Genetics, University of Cambridge, Cambridge, United Kingdom

⁸Massachusetts Eye and Ear Infirmary, Ocular Genomics Institute, Boston, Massachusetts, United States

⁹Harvard Medical School, Boston, Massachusetts, United States

¹⁰Department of Ophthalmology, St. Thomas' Hospital, London, United Kingdom

¹¹Department of Ophthalmology, National University of Singapore, Singapore

¹²Department of Pediatrics, Section of Medical Genetics, West Virginia University, Morgantown, West Virginia, United States

Correspondence: Andrew R. Webster, Moorfields Eye Hospital, 162 City Road, London EC1V 2PD, United Kingdom; andrew.webster@ucl.ac.uk.

Gavin Arno, UCL Institute of Ophthalmology, 11-43 Bath Street, London EC1V 9EL, United Kingdom; g.arno@ucl.ac.uk.

GA and ARW contributed equally to the work presented here and should therefore be regarded as equivalent authors.

Submitted: June 14, 2018

Accepted: August 18, 2018

Citation: Ba-Abbad R, Leys M, Wang X, et al. Clinical features of a retinopathy associated with a dominant allele of the *RGR* gene. *Invest Ophthalmol Vis Sci.* 2018;59:4812–4820. <https://doi.org/10.1167/iovs.18-25061>

PURPOSE. We describe the clinical features in two pedigrees with dominantly inherited retinopathy segregating the previously reported frameshifting mutation, c.836dupG (p.Ile280Asn*78) in the terminal exon of the *RGR* gene, and compare their haplotypes to that of the previously reported pedigree.

METHODS. The probands were ascertained at West Virginia University Eye Institute (WVU) and Moorfields Eye Hospital (MEH) through next generation sequencing (NGS) and whole genome sequencing (WGS) respectively. Clinical data included visual acuity (VA), visual fields, fundus autofluorescence (FAF), optical coherence tomography (OCT), and electroretinography (ERG). Haplotype analysis was performed using Sanger sequencing of the DNA from the molecularly ascertained individuals from the three pedigrees.

RESULTS. Nine heterozygous mutation carriers were identified in two families. Four carriers were asymptomatic; five carriers had variable VA reduction, visual field constriction, and experienced difficulty under dim illumination. Fundus examination of the asymptomatic carriers showed diffuse or reticular pigmentation of the retina; the symptomatic carriers had chorioretinal atrophy. FAF imaging showed widespread signal loss in advanced retinopathy, and reticular hyperautofluorescence in mild cases. OCT showed loss of outer retinal lamina in advanced disease. ERG showed moderate-to-severe rod-cone dysfunction in two symptomatic carriers; and was normal in three asymptomatic carriers. A shared haplotype flanking the mutation of up to 6.67 Mb was identified in both families. Within this region, 1.27 Mb were shared with the first family reported with this retinopathy.

CONCLUSIONS. The clinical data suggest a variable and slow degeneration of the RPE. A shared chromosomal segment surrounding the *RGR* gene suggests a single ancestral mutational event underlying all three families.

Keywords: autosomal dominant retinal dystrophy, deep retinal reticular pigmentation, next generation sequencing, whole genome sequencing, *RGR*

Inherited retinal dystrophies are a group of disorders in which retinal dysfunction and/or degeneration is due to disease-causing variants in one or both alleles of a single gene. They present with variable clinical features, and have high genetic and allelic heterogeneity. To date, disease-causing variants in more than 300 genes have been identified (available in the public domain at <https://sph.uth.edu/retnet/>; The University of

Texas-Houston Health Science Center, Houston, TX, USA). Proteins encoded by these genes can be expressed ubiquitously, or by specific retinal cell types.^{1–4}

The retinal G-protein coupled receptor gene (*RGR*, MIM_600342) is located on chromosome 10q23.1, and encodes an intracellular opsin localized to the retinal pigment epithelium (RPE) and Müller cells.^{5–7} To date, only one disease-causing



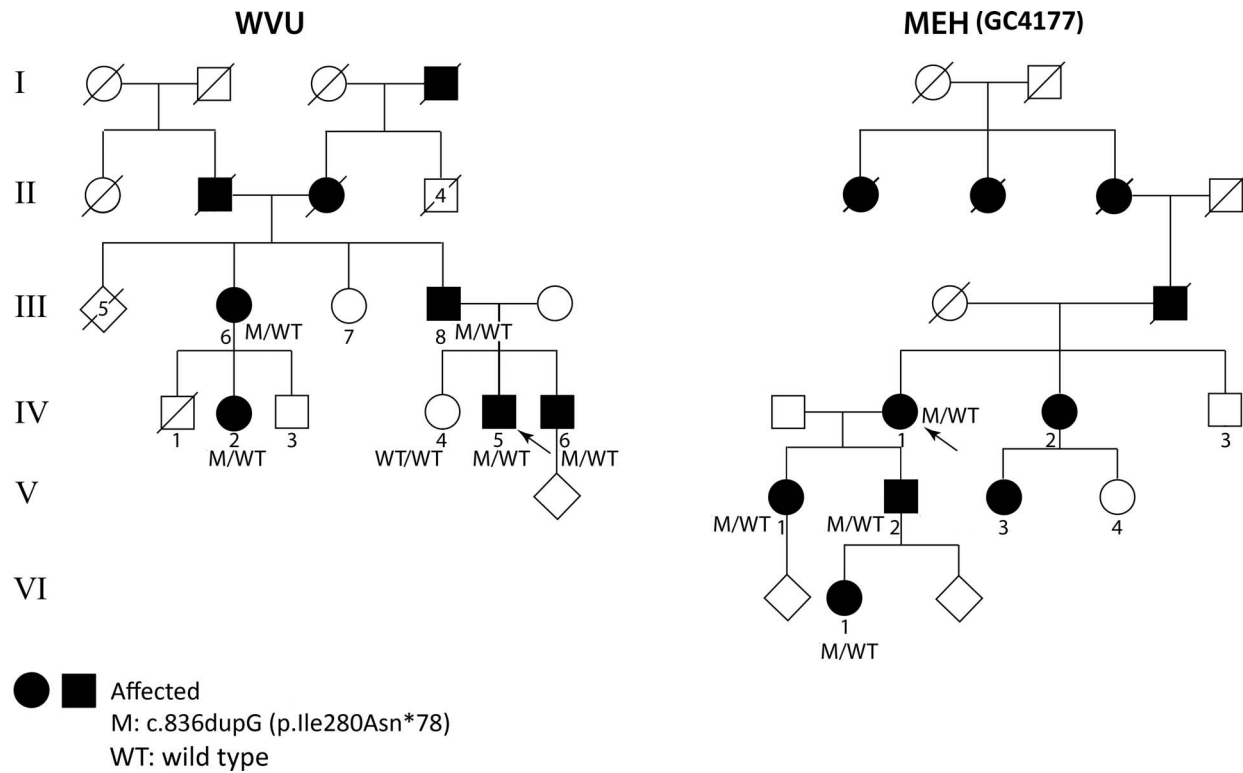


FIGURE 1. Pedigrees of the families from WVU and MEH-GC4177. Subjects with history of blindness in WVU: I, II, and MEH II, III, and IV are shown as *solid symbols*. In both pedigrees, all the genotyped members (denoted as M/WT for heterozygotes and WT/WT for those with wild type alleles) were examined and retinal images were obtained. Subjects WVU: IV-2, IV-5; and MEH-GC4177: V-2, VI-1 had distinct retinal changes on imaging but no visual symptoms. *Arrows* indicate the proband in each family.

mutation in *RGR* has been described: a heterozygous frameshift mutation (chr10:86018343dupG; NM_002921.3:c.836dupG; p.Ile280Asn*78 — the same mutation as reported previously), which was reported in a pedigree with autosomal dominant retinopathy, but the clinical data were limited (RP44; MIM-613769).⁸ An allele reported to be associated with recessive retinal disease has been re-evaluated, with the disorder in those patients explained, instead, by biallelic mutation of *CDHR1*.⁹ Therefore, the consequences of biallelic loss of function of *RGR* on the human retina remain unknown.⁹ We characterized the clinical features secondary to the frameshifting mutation p.Ile280Asn*78 in *RGR* in two not knowingly related Caucasian pedigrees from the United Kingdom and United States.

METHODS

Two probands (shown by arrows in Fig. 1) were initially ascertained through large sequencing studies. Family WVU was recruited from the medical retina clinic at the West Virginia University Eye Institute (WVU); family GC4177 was recruited from the inherited retinal disorders clinic at Moorfields Eye Hospital (MEH; Fig. 1). After obtaining informed consent, the probands and their family members donated blood for genetic testing. DNA analysis from the WVU family was performed as part of the National Ophthalmic Disease Genotyping and Phenotyping Network (eyeGENE) study, as a Health Insurance Portability and Accountability Act (HIPAA)-compliant study that was approved by the institutional review boards at WVU, and the National Eye Institute (Bethesda, MD, USA). DNA analysis from the GC4177 family was performed as part of the National Institute for Health Research BioResource-Rare Diseases (NIHRBR-RD) study, which was approved by

MEH Research Management Ethics, and Cambridge South Research Committee, and adhered to the tenets of the Declaration of Helsinki. Details of the molecular investigations at WVU and MEH, including the haplotype analysis from the two pedigrees and the family reported by Morimura et al.,⁸ are provided in the Supplementary Material.

Sanger sequencing of all coding exons and exon-intron boundaries of *RGR* in 18 unrelated probands from MEH, whose retinal features were similar to those of the MEH proband and WVU: III-8, and were negative for *CHM* mutations, did not identify further carriers of this change or other likely disease-causing variants in *RGR* (primers available upon request).

The probands and available family members underwent ophthalmic examination including best-corrected Snellen visual acuity (VA), dilated fundus examination, optical coherence tomography (OCT), fundus autofluorescence (FAF) imaging (Spectralis HRA+OCT; Heidelberg Engineering GmbH, Heidelberg, Germany), color fundus photography, Goldmann perimetry, and electrophysiologic testing using protocols that incorporated the recommendations of the International Society of Electrophysiology of Vision (ISCEV) for electroretinography (ERG), pattern electroretinography (PERG), and electrooculography (EOG) at the time of examination.¹⁰⁻¹²

RESULTS

Molecular Genetic Analysis

A previously reported⁸ heterozygous variant in *RGR* (NM_002921.3 c.836dupG; p.Ile280Asnfs*78, MIM_600342.0002) was detected in the genomic DNA from both probands WVU-IV:5, and GC4177-IV:1 by targeted next generation sequencing (NGS) and whole genome sequencing (WGS), respectively.

TABLE 1. Whole Genome Sequencing Data for the Proband GC4177-IV-1

VAR (hg19)	rs Number	Reference	Allele Frequency	GC4177	WVU	Morimura et al. ⁸
10:81305881	rs149240458	C	0.0001	T	T	C
<i>10:85446602</i>	<i>rs186897671</i>	<i>C</i>	<i>0.009</i>	<i>T</i>	<i>T</i>	<i>T</i>
<i>10:85711138</i>	<i>rs61868868</i>	<i>C</i>	<i>0.13</i>	<i>A</i>	<i>A</i>	<i>A</i>
<i>10:85711734</i>	<i>rs35868777</i>	<i>T</i>	<i>0.14</i>	<i>C</i>	<i>C</i>	<i>C</i>
10:86018343	..	A	NA	AG	AG	AG
<i>10:86713933</i>	<i>rs577984121</i>	<i>A</i>	<i>0.00019</i>	<i>AC</i>	<i>AC</i>	<i>AC</i>
10:87978214	rs4934162	G	0.047	A	A	G
10:87979761	rs4934163	T	0.047	C	C	T
10:90244571	rs750593376	CAG	0.00003	C	CAG	CAG

Heterozygous for the c.836dupG Mutation in *RGR* (VAR [hg19] position: 10: 86018343, shown in bold font), were interrogated in the regions >2 Mb telomeric and centromeric to the mutation. All high-quality single-nucleotide polymorphisms (SNPs) with a reference ID in the refSNP cluster (rs), and an allele frequency of the nonreference allele of <0.2 on gnomAD (available in the public domain at <http://gnomad.broadinstitute.org>; the Broad Institute) were identified. DNA from the unaffected father IV-2, and affected children V-1 and V-2 underwent Sanger sequencing of 32 SNPs to determine the phase relative to the maternally inherited mutation. In eight of these, the phase could be unambiguously determined showing each to segregate with the *RGR* mutation. These SNPs were examined by Sanger sequencing in affected members of the other two families. These data supported a minimal shared haplotype of 1.27 Mb across the three pedigrees (SNPs, shown in italicized font).

Direct Sanger sequencing of the DNA from available family members from both pedigrees (Fig. 1; WVU: III-6, III-8, IV-2, IV-5, IV-6, and GC4177: V-1, V-2, and VI-1) demonstrated the variant to be present in the DNA from all of these individuals, and segregate with retinal changes on fundus examination; WVU: IV-4 had normal ocular examination and the wild type allele. Haplotype analysis using 32 single nucleotide variants (SNV), with a minor allele frequency (MAF) of <0.2 in the gnomAD dataset (available in the public domain at <http://gnomad.broadinstitute.org>; Broad Institute, Cambridge, MA, USA), selected from the WGS data of GC4177: IV-1 showed eight SNVs to be shared between the following subjects: GC4177: V-1, V-2 and WVU: IV-5, IV-6 (Table 1), indicating a shared haplotype region of 6.67 Mb inclusive of *RGR* (primers available upon request). Additional Sanger sequencing of the DNA from three affected and two unaffected family members from the first pedigree, which was reported by Morimura et al.,⁸ for the eight shared SNVs showed a common haplotype of 1.27 Mb across the three pedigrees.

The variant, a duplication of a single nucleotide (G) at position 836 in exon 7 of *RGR*, is predicted to result in an out-of-frame extension through the canonical stop codon, producing a longer polypeptide with 77 novel amino acid residues at the C-terminal end, and replacing 16 amino acid residues in the cytoplasmic domain of *RGR*. Because the variant is in the terminal exon of *RGR*, the transcript is likely to evade nonsense mediated decay and a mature protein could be produced.

Clinical Features

The clinical, visual function and imaging data are summarized in Table 2. Nine subjects were examined, five from two generations in the WVU pedigree and four from three generations in the GC4177 pedigree (Fig. 1). No other family members were available for examination. Median age of the asymptomatic carriers with normal visual acuity was 50 years (range, 23–60 years). There was no contributory medical or drug history.

The earliest symptoms in WVU: III-8 were visual field defects and reduced VA at the age of 59 years. WVU: III-6 had visual field defects and mildly reduced VA at the age of 81 years. Subjects GC4177: IV-1 and GC4177: V-1 first noticed progressive visual field constriction during their third decade of life. The VA in symptomatic carriers ranged between 20/20 and 20/1000. WVU III-8 had a VA of 20/50 in the right eye and 20/200 improving with pinhole to 20/50 in the left eye at the

age of 77 years, but GC4177: IV-1 suffered severe VA loss during the seventh decade. Not all subjects were available for refraction (Table 2). All three carriers from the WVU pedigree whose visual fields were available showed enlargement of the blind spot. Additionally, one carrier had bilateral nasal and temporal scotomata.

Fundus examination of subjects WVU: III-8 and III-6 at ages 77 and 81 years, respectively, and GC4177: IV-1 at age 73 years showed increased visibility of the large choroidal blood vessels, in keeping with loss of the RPE, without significant attenuation of the retinal blood vessels (Figs. 2, 3). Two subjects showed discrete patches of deep retinal hyperpigmentation: WVU: III-6 (Fig. 2D, green arrow) and GC4177: IV-1 (Fig. 3A, green arrows). Subject GC4177: V-1 showed only peripapillary atrophy, but the deep retinal changes became conspicuous on FAF imaging as described below. The asymptomatic carriers (WVU: IV-2, IV-5, IV-6 and GC4177: V-2, VI-1) showed, in addition to peripapillary atrophy, bilateral deep retinal pigmentation anterior to the vascular arcades (Figs. 2G, 2J) and nasal to the optic disc (Fig. 3G). Subject GC4177: V-2 showed peripapillary atrophy extending toward the fovea (Fig. 3G).

FAF imaging showed sharply demarcated areas of hypoautofluorescence in advanced cases. The areas of relatively preserved outer retina had mottling of the AF or reticular hyperautofluorescence (Figs. 2B, 2E, 3B, 3E). The changes were more noticeable on FAF than on color fundus imaging, with FAF showing reticular hyperautofluorescence and patches of reduced AF (Figs. 2E, 2H, 2K, 3H).

OCT showed marked disruption of the inner segment–outer segment junction band (IS/OS) in advanced cases (WVU: III-8 and GC4177: IV-1) with attenuation of the outer nuclear layer (Figs. 2C, 3C). Outer retinal tubulation was present at the junction between the atrophic fovea and a layer resembling the IS/OS (Fig. 3C, red arrow) or temporal to the optic nerve head (Figs. 3I, 3L). Subject WVU: III-6 showed preservation of the central foveal structure on OCT, separated from the nasal, atrophic region by a hyporeflexive band reminiscent of an interlamellar bridge (Fig. 2F, yellow arrow). Subject GC4177: V-1 showed mild IS/OS irregularity on OCT (Fig. 3F, cyan arrow). The asymptomatic carriers showed attenuation or loss of the photoreceptor layer in the peripapillary area (Figs. 2I, 2H, 3I). Foveal lamination was normal in all asymptomatic carriers.

Electroretinography was available for three subjects from the WVU pedigree—data given in Supplementary Table S1 and waveforms in Figure 4 (one subject also had an EOG)—and two subjects from the GC4177 pedigree (Fig. 5). The

TABLE 2. Clinical Features of RGR Retinopathy in Two Unrelated Pedigrees

Subject; Age, y	Presentation	BCVA	Visual Field	Fundus Features	FAF	OCT	ERG
WVU: III-6; 81	Visual field defects	RE: 20/30; LE: 20/25 RE: -1.00+0.75 × 175 LE: -0.50 DS	Enlarged blind spots, BE	Bilateral peripapillary atrophy	Reduced peripapillary AF, extending nasally & temporally, relative foveal sparing, reticular pattern of increased AF in the posterior pole, speckled AF inferiorly	Relative sparing of the fovea, interlaminar bridge nasal to the fovea, peripapillary loss of outer retinal layers, thin choroid	Moderate-to-severe reduction of scotopic and photopic responses
WVU: III-8; 59	Reduced VA	RE: 20/25; LE: 20/60 RE: +0.75+1.00 × 145 LE: -0.50+1.75 × 175	Enlarged blind spot & large nasal scotomata, BE	Extensive peripapillary atrophy, relative foveal sparing. At age 77: bilateral chorioretinal atrophy in the posterior pole	Reduced AF with islands of preserved AF in the posterior pole	At age 77: interlaminar bridge temporal to the fovea; extensive loss of the outer retina, thin choroid	Moderate reduction of scotopic bright flash response; mildly subnormal photopic b-wave amplitude
WVU: IV-2; 60	Asymptomatic	RE: 20/20; LE: 20/20	NA	Bilateral peripapillary atrophy & peripheral reticular pigmentation	Reduced peripapillary AF; reticular pattern of increased AF; sparing of the posterior pole.	Preservation of the foveal structure, peripapillary loss of outer retinal layers	NA
WVU: IV-5; 50	Asymptomatic; peripapillary atrophy	RE: 20/20; LE: 20/20 RE: +0.75+0.75 × 132 LE: +1.00+0.50 × 37	Enlarged blind spots, BE	Bilateral peripapillary atrophy & peripheral reticular pigmentation	Reduced peripapillary AF; reticular pattern of increased AF and patches of reduced AF nasally	Preservation of the foveal structure, deep peripapillary excavation & loss of outer retinal layers	Normal scotopic & photopic responses
WVU: IV-6; 48	Difficulty driving at night	RE: 20/25; LE: 20/25	NA	Bilateral peripapillary atrophy & peripheral reticular pigmentation	NA	NA	NA
MEHGC4177: IV-1; 73	Reduced VA, difficulty seeing under dim light, & visual field defects	RE: 20/1000; LE: 20/80	NA	Bilateral chorioretinal atrophy, no retinal vascular attenuation, patches of intraretinal pigmentation in the temporal periphery	Widespread reduced AF with islands of preserved AF in the posterior pole	Extensive loss of the outer retina at the posterior pole; ORT	NA
MEHGC4177: V-1; 52	Progressive visual field constriction	RE: 20/20; LE: 20/30	NA	Bilateral peripapillary atrophy & peripheral reticular pigmentation	Reduced peripapillary AF; reticular AF pattern, patches of reduced AF nasally, relative sparing of the parafoveal region	Mild disruption of the EZ & the IZ; focal thickening of the RPE band nasal to the fovea	NA
MEHGC4177: V-2; 51	Asymptomatic	RE: 20/20; LE: 20/20	NA	Bilateral peripapillary atrophy & peripheral reticular pigmentation	Reduced peripapillary AF; reticular pattern of increased AF nasally	Marked attenuation of the ONL & EZ nasal to the fovea; ORT	Normal scotopic & photopic responses
MEHGC4177: VI-1; 23	Asymptomatic	RE: 20/15 LE: 20/20	Normal	Bilateral peripapillary atrophy & diffuse retinal pigment alteration	Reduced peripapillary AF; widespread "salt-and-pepper" hypo-AF anterior to the vascular arcades	Preservation of the foveal structure, peripapillary loss ONL & EZ; ORT	Normal scotopic & photopic responses

Patients were examined at WVU or MEHGC4177. BCVA, best-corrected visual acuity; RE, right eye; LE, left eye; BE, both eyes; DS, spherical diopter; FAF, fundus autofluorescence; AF, autofluorescence; OCT, optical coherence tomography; EZ, ellipsoid zone; IZ, inter-digitation zone; RPE, retinal pigment epithelium; ONL, outer nuclear layer; ORT, outer retinal tubulation; ERG, full-field electroretinogram; NA, not available.

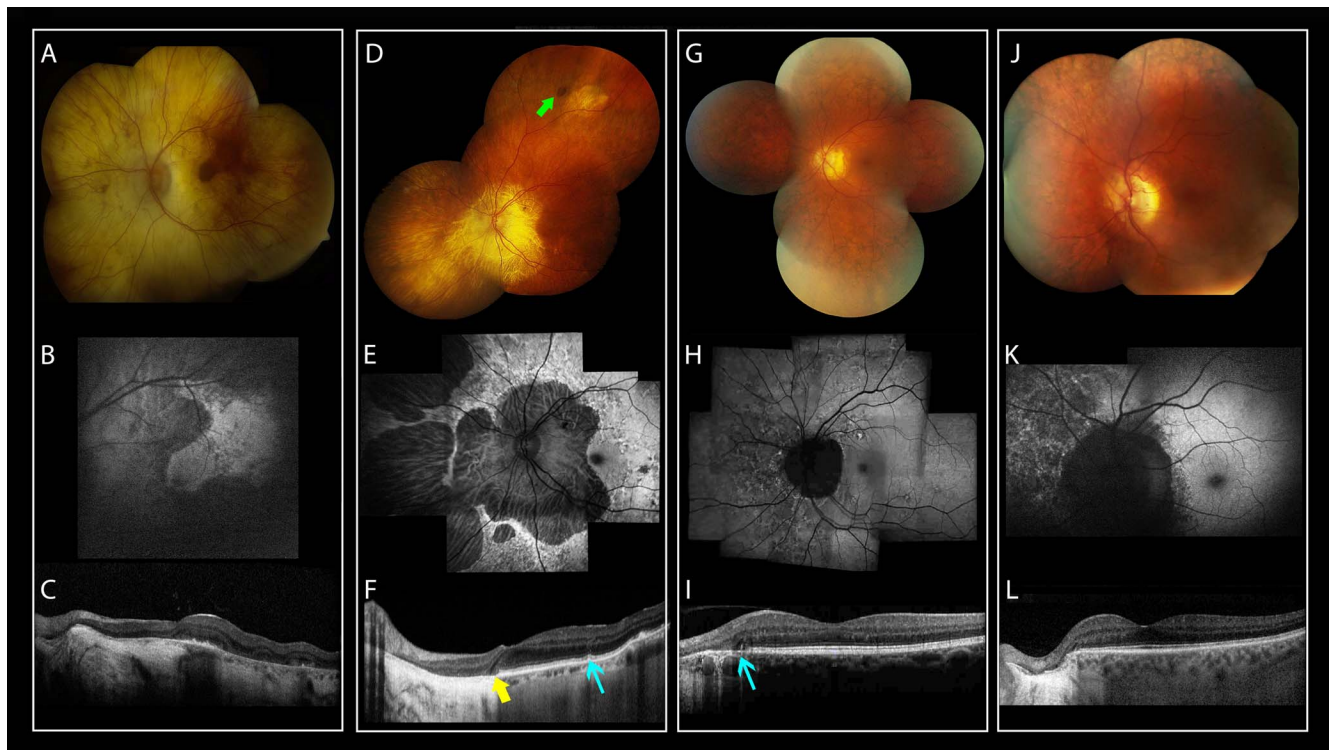


FIGURE 2. Retinal images for the carriers of the c.836dupG mutation in *RGR* from the WVU pedigree. Color fundus photographs (A, D, G, J), FAF (B, E, H, K), and OCT scans (C, F, I, L) for individuals from the WVU pedigree harboring the c.824dupG mutation in *RGR*, each column shows images for one individual. (A–C) Images for patient III-8 showing: (A) diffuse chorioretinal atrophy, with partial preservation of the fovea (note the lack of intraretinal pigment migration); (B) FAF of the posterior pole showing an island of preserved, yet mottled signal; (C) OCT shows loss of the ellipsoid zone (EZ) in the entire scan except for a small area under the fovea, with marked attenuation of the outer nuclear layer (ONL); the choroidal blood vessels are nearly absent. (D–F) images for patient III-6 showing: (D) extensive peripapillary atrophy, and an isolated patch of intraretinal pigmentation (green arrow); (E) FAF shows loss of AF extending in the nasal retina, and a reticular pattern in the posterior pole with foveal sparing; (F) OCT shows an intralaminar bridge (yellow arrow) demarcating the edge of the preserved outer retina; focal excrescence of the RPE band is shown in the region of the reticular changes (cyan arrow). (G–I, J–L) Images for patients IV-5 and IV-6, showing peripapillary atrophy and reticular pigmentation (G, J), peripapillary hypoautofluorescence and reticular changes nasal to the optic disc (H, K), sharp demarcation on OCT between the atrophic and preserved retina (I, L, see cyan arrow in I).

asymptomatic carriers WVU: IV-5 (note the normative data in Supplementary Table S2) and GC4177: V-2, VI-1 had normal scotopic and photopic full field ERGs. The PERG was normal in the youngest carrier GC4177:VI-1, but showed mildly reduced P50 amplitude in GC4177: V-2. Subjects WVU: III-6 and WVU: III-8 were symptomatic, and the ERG from WVU: III-6 showed moderately severe reduction of the scotopic amplitudes at the age of 81 years, with delayed and subnormal photopic responses. The ERG recordings from WVU: III-8 (at the age of 59 years with limited outer retinal atrophy) showed moderate reduction of the scotopic bright flash response; and subnormal photopic b-wave amplitude with normal peak time, in addition to mild reduction of the EOG light rise (light peak-dark trough ratio of 1.6) in both eyes. Because of the putative role of *RGR* in the visual cycle,¹³ ERG was performed in subject GC4177: V-2 after extended monocular dark adaptation overnight. The amplitude of the scotopic mixed bright flash response of the eye that underwent extended dark adaptation was higher than that of the eye that underwent standard dark adaptation for 20 minutes, but this difference was not clinically significant.

DISCUSSION

We described the clinical features of retinal dystrophy associated with a rare, heterozygous frameshifting mutation in *RGR* in two families from the United States and the United

Kingdom with a haplotype that is shared with the first reported family,⁸ and demonstrated the spectrum of retinal changes. These ranged from seemingly innocuous reticular or diffuse deep retinal pigment alteration, normal visual acuity, and normal ERG, to diffuse atrophy of the retina and choroid with severe visual loss. Longitudinal data for the asymptomatic carriers were limited and, therefore, it is unknown if the retinal changes in those subjects are nonprogressive signs of the carrier state or represent an early stage of a slowly progressive retinal dystrophy. The features of *RGR*-retinopathy emphasize the importance of FAF imaging in recognizing mild retinal manifestations and guiding the molecular investigation in individuals with poor vision under dim lighting conditions and peripapillary RPE atrophy. Variable expressivity (variable phenotypic severity) and low penetrance (mutation carriers with no associated phenotype) also have been observed in pedigrees heterozygous for the p.Asp477Gly allele in *RPE65*, another dominant disease affecting the RPE.¹³

In the first report of *RGR* retinopathy, the proband showed bilaterally subnormal VA, macular atrophy, and severely reduced ERGs, but the milder and early manifestations of this retinopathy were not described.⁸ The clinical features of retinal dystrophies with presumed primary RPE pathology differ from those of retinitis pigmentosa by the paucity of intraretinal bone spicule pigment deposition, and relative preservation of the retinal vascular caliber. The phenotype described in patients WVU: III-8 and GC4177: IV-1 resembles

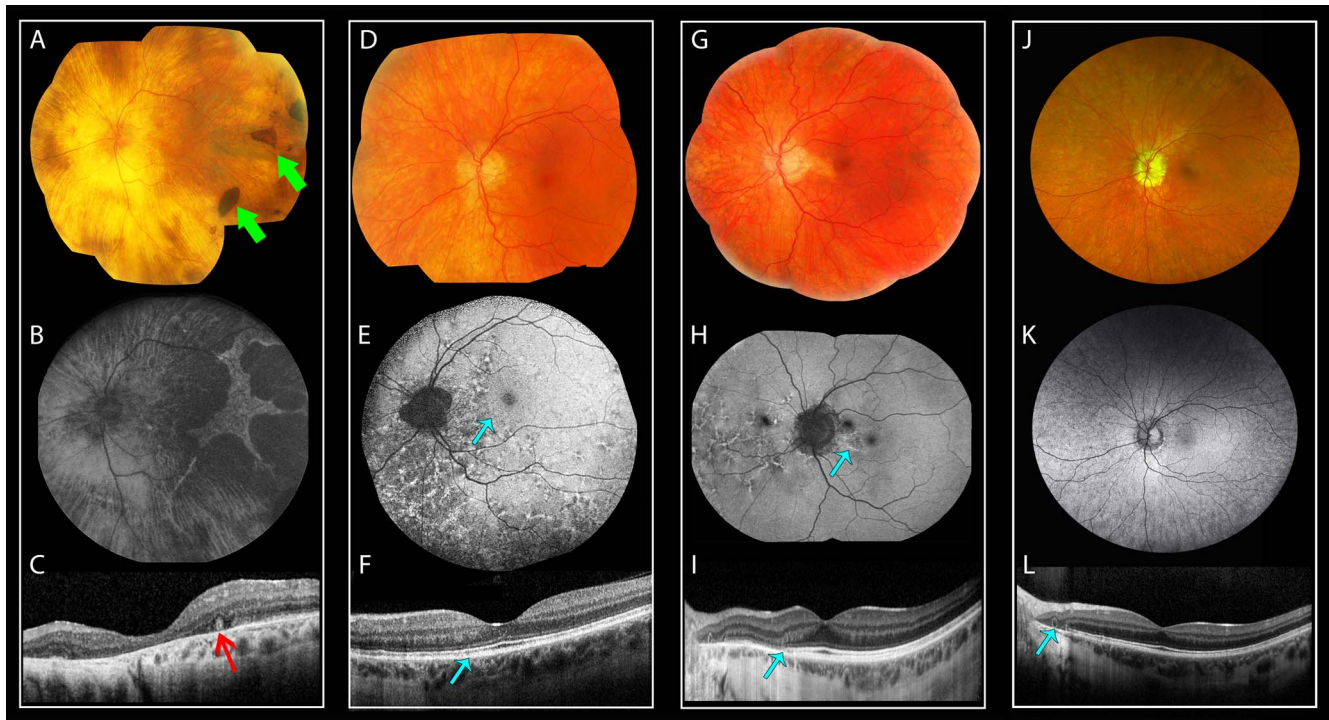


FIGURE 3. Retinal images for the carriers of the c.836dupG mutation in *RGR* from the MEH pedigree. Color fundus photographs (A, D, G), FAF (B, E, H), and OCT images (C, F, I) for individuals from the GC4177 family carrying the c.824dupG mutation in *RGR*. (A–C) Images for the proband IV-1 showing (A) diffuse chorioretinal atrophy, patches of intraretinal pigmentation (green arrows) are noted in the temporal retina; (B) FAF shows diffuse loss of AF except for an island with scalloped edges temporal to the fovea; (C) OCT shows outer retinal tubulation (ORT; red arrow). (D–F) Images for patient V-1. (D) Deep reticular pigmentation in the nasal retina. (E) FAF shows peripapillary atrophy and reticular changes in the nasal retina, note the edge nasal to the fovea corresponding to the subtle irregularity of the ellipsoid zone and RPE bands on OCT (F), cyan arrow). (G–I) Fundus images for the asymptomatic carrier V-2 showing (G) peripapillary atrophy and reticular pigmentation nasal to the optic disc and temporal to the macula. (H) Outer retinal atrophy extending toward the fovea (cyan arrow), and reticular AF pattern nasal to the disc. (I) OCT showing attenuation of the ONL and EZ nasal to the fovea. Note the ORT temporal to optic nerve head. (J–L) fundus images of the asymptomatic carrier VI-1. (J) peripapillary atrophy and diffuse deep retinal pigmentation anterior to the vascular arcades, better visualized on FAF (K). (L) OCT showing absence of the ONL and EZ temporal to the optic nerve head; note also the ORT (cyan arrow).

that observed in choroideremia (CHM), patients heterozygous for the p.Asp477Gly mutation in *RPE65*, some *PRPH2* mutations, and the p.M216K mutation in *RHO*.^{15–16} CHM, and *RPE65*- and *RGR*-dominant retinopathies affect initially the RPE due to the expression of their respective genes, and, therefore, are likely to have similar clinical features. Early RPE involvement in some cases of *PRPH2*-retinopathy and the p.M216K mutation in *RHO* remain unexplained as both genes are expressed in the photoreceptors.^{15,16} One early symptom common to these disorders is reduced vision in the dark; it is plausible to speculate that the impaired night vision is caused by an abnormal visual cycle in the affected RPE while the cone function is spared due to the Müller cell-mediated visual cycle.¹⁷

Electrophysiologic testing in one individual with advanced retinopathy showed loss of retinal function without shifting the peak-time, suggesting that the main pathology in some cases is loss of photoreceptor function without dysfunction. The subnormal EOG in this patient can be associated with reduction of the scotopic ERG and is milder than the reported abolished EOG light rise in a patient with a similar retinal phenotype in dominant RPE dystrophy due to the p.Asp477Gly allele in *RPE65*.¹⁵ *RGR* and *RPE65* are expressed in the RPE and these alleles likely result in cellular toxicity.^{5,13,18} The subnormal macular function, as shown on PERG in one asymptomatic carrier, suggested that this retinopathy can involve the macula.

To date, there are no other known disease-causing mutations in *RGR*. It is informative to examine the population variants in the gnomAD database (available in the public domain at <http://gnomad.broadinstitute.org/gene/ENSG00000148604>; the Broad Institute). The presence of numerous predicted loss of function mutations suggests that haploinsufficiency is too common to be responsible for retinal disease and supports our hypothesis that the reported allele has a toxic or gain-of-function effect. Moreover, eight instances of one specific final exon frame-shifting mutation in 24028 African alleles also are present (NM_002921.3:c.796_797insCC; p.Ile267Profs*37; rs770085833). No other C-terminal frame-shifting alleles are reported. The c.796_797insCC variant, unlike the c.836dupG variant reported in our study, affects the noncanonical reading-frame and produces a different carboxyl terminal peptide (by an out-of-frame extension through the canonical stop codon, adding seven novel amino-acids at the carboxyl terminal, and replacing 29 amino-acids in the cytoplasmic domain of RGR). In addition to containing distinct amino-acids, it also is shorter than that predicted from the c.836dupG variant. This observation further supported the assertion that the retinopathy reported here is due to toxicity conferred by the specific abnormal carboxyl peptide.

The shared haplotype, in the three pedigrees, suggests that the p.Ile280Asnfs*78 allele is a founder mutation. Recognition of this phenotypic variability could lead to identification of further affected families, and analysis of their respective haplotypes.

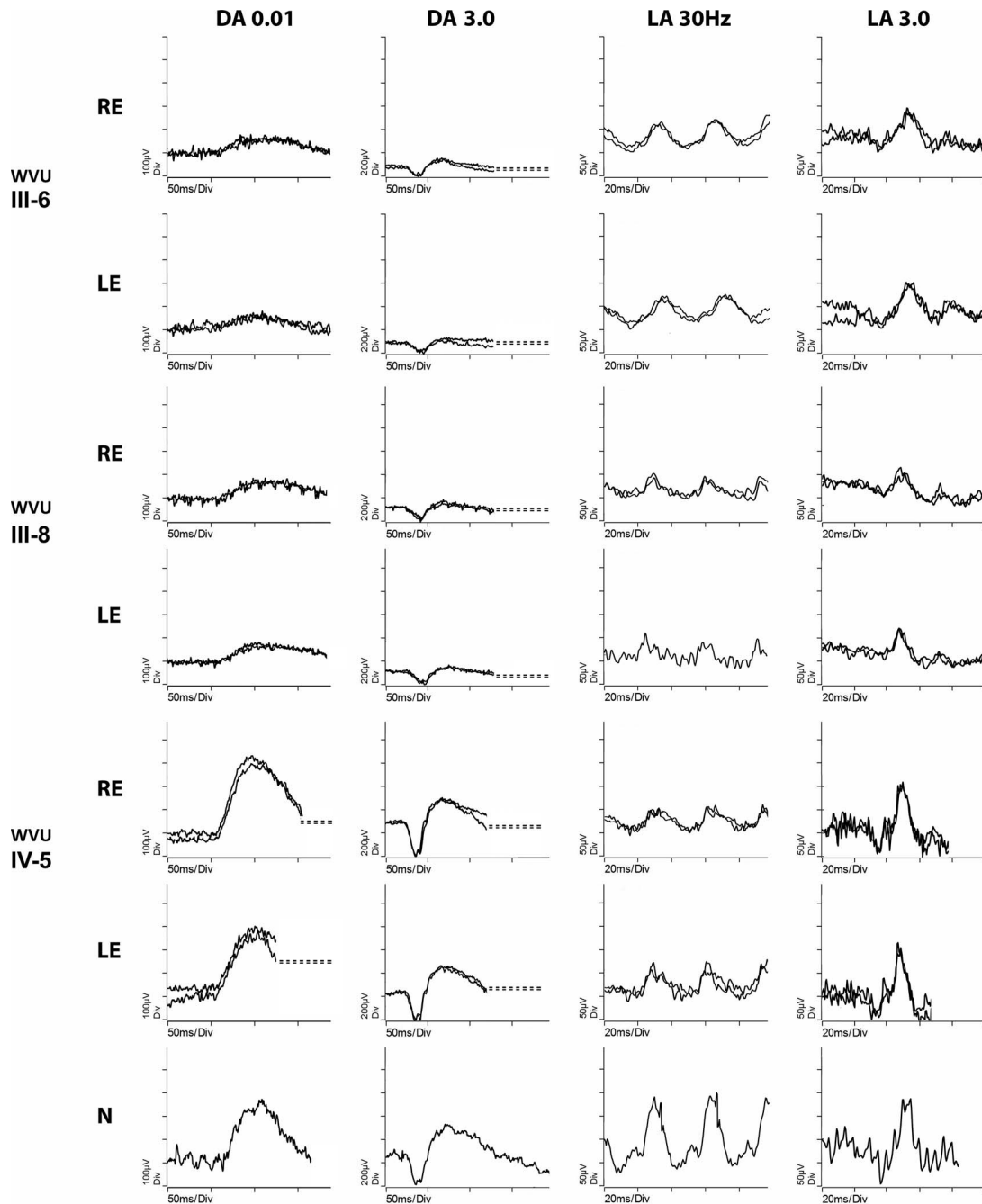


FIGURE 4. ERG for three carriers of the c.824dupG mutation in *RGR*: data for WVU: III-6, WVU: III-8, and WVU: IV-5, are presented with responses recorded from a healthy 58-year control in the bottom for comparison. Note that the recording was performed according to the previous ISCEV standard protocols, which have been updated after the recordings were obtained. The WVU age-matched normative data are given in Supplementary Table S2. DA 0.01: dark adapted response to a dim flash stimulus (0.01 cd.s.m^{-2}); DA 3.0: dark adapted response to a bright flash stimulus (3.0 cd.s.m^{-2}); LA 30Hz: light adapted response to a 30 Hz flicker stimulus with intensity 3.0 cd.s.m^{-2} ; LA 3.0: light adapted response to a flash stimulus (3.0 cd.s.m^{-2}). Note the electrical noise resulting from the mains interference.

Our study reinforced the notion that, although candidate gene testing—when a distinct phenotype is observed—often is helpful, unbiased genetic screening using large NGS panels or whole exome/genome sequencing can reveal unexpected genotype–phenotype associations and expand the list of candidate genes.^{19,20}

In conclusion, this report exemplified the success of the unbiased approaches of WGS and NGS in the molecular diagnosis of a highly genetically heterogeneous disorder, such as retinal dystrophy. The clinical features suggested a variable

severity of retinopathy consequent upon heterozygosity of a specific allele of the *RGR* gene. The slow progression of this retinopathy and possible primary involvement of the RPE make this disorder tractable to potential therapeutic interventions.

Acknowledgments

The authors thank Beverley Scott, from UCL Institute of Ophthalmology, for performing the DNA extraction, Maisie E.

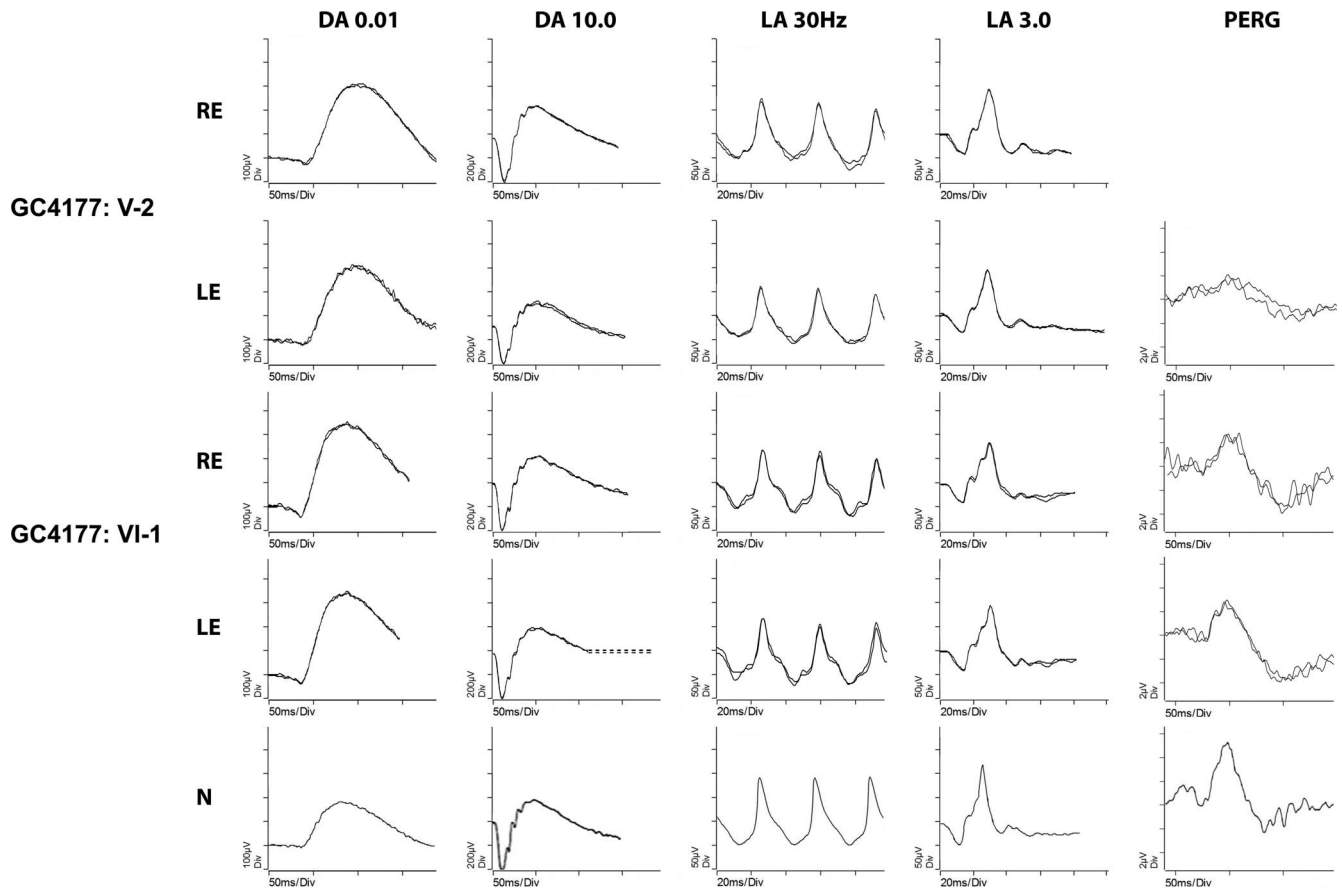


FIGURE 5. ISCEV-standard ERG for two carriers of the c.824dupG mutation in *RGR*: GC4177: V-2 and GC4177: VI-1, together with responses recorded from a healthy control in the bottom for comparison. RE, right eye; LE, left eye. DA 0.01: dark adapted response to a dim flash stimulus (0.01 cd.s.m^{-2}); DA 10.0: dark adapted response to a bright flash stimulus (10.0 cd.s.m^{-2}); LA 30Hz: light adapted response to a 30 Hz flicker stimulus with intensity 3.0 cd.s.m^{-2} ; LA 3.0: light adapted response to a flash stimulus (3.0 cd.s.m^{-2}); PERG: pattern ERG response to a standard 15° field. The full field and PERG for VI-1 are normal. The right eye of V-2 underwent extended dark adaptation before ERG testing to investigate if the *RGR* mutation affects the visual cycle. The amplitude of the dark-adapted response to DA 10.0 from the right eye is higher than that from the left eye, but this difference is not clinically significant. The scotopic and photopic full field ERGs from both eyes are normal. PERG shows mild reduction of the P50 amplitude in the left eye, with normal peak time.

Punt, and Samantha Malka from MEH for the administrative support, and Priya Francome-Wood, from MEH for the genetic counseling service.

Supported by Diana Davis Spencer Clinical Fellowship from the Foundation Fighting Blindness-USA; NIHR Biomedical Research Centre at Moorfields Eye Hospital (RB); Foundation Fighting Blindness-USA (GEH); Research to Prevent Blindness unrestricted challenge grant (WVU Eye Institute); EyeGENE, National Institutes of Health/National Eye Institute extramural clinical and intramural programs (XW); Wellcome Trust (OAM; Grant 206619/Z/17/Z); Fight for Sight UK; Fight for Sight UK - Early Career Investigator Award (GA); NIHR Biomedical Research Centre at Moorfields Eye Hospital, UCL Institute of Ophthalmology (GEH, OAM, GA) and Cambridge; and the NIHR Bioresource for Rare Diseases.

Disclosure: **R. Ba-Abbad**, None; **M. Leys**, None; **X. Wang**, None; **C. Chakarova**, None; **N. Waseem**, None; **K.J. Carss**, None; **F.L. Raymond**, None; **K.M. Bujakowska**, None; **E.A. Pierce**, None; **O.A. Mahroo**, None; **M.D. Mohamed**, None; **G.E. Holder**, None; **M. Hummel**, None; **G. Arno**, None; **A.R. Webster**, None

References

1. Bech-Hansen NT, Naylor MJ, Maybaum TA, et al. Mutations in NYX, encoding the leucine-rich proteoglycan nycalopin, cause X-linked complete congenital stationary night blindness. *Nat Genet.* 2000;26:319-323.
2. Dryja TP, McGee TL, Reichel E, et al. A point mutation of the rhodopsin gene in one form of retinitis pigmentosa. *Nature.* 1990;343:364-366.
3. Kohl S, Zobor D, Chiang WC, et al. Mutations in the unfolded protein response regulator ATF6 cause the cone dysfunction disorder achromatopsia. *Nat Genet.* 2015;47:757-765.
4. Chakarova CE, Papaioannou MG, Khanna H, et al. Mutations in TOPORS cause autosomal dominant retinitis pigmentosa with perivascular retinal pigment epithelium atrophy. *Am J Hum Genet.* 2007;81:1098-1103.
5. Jiang M, Pandey S, Fong HK. An opsin homologue in the retina and pigment epithelium. *Invest Ophthalmol Vis Sci.* 1993;34:3669-3678.
6. Chen XN, Korenberg JR, Jiang M, et al. Localization of the human RGR opsin gene to chromosome 10q23. *Hum Genet.* 1996;97:720-722.
7. Pandey S, Blanks JC, Spee C, et al. Cytoplasmic retinal localization of an evolutionary homolog of the visual pigments. *Exp Eye Res.* 1994;58:605-613.
8. Morimura H, Saindelle-Ribeaud F, Berson EL, Dryja TP. Mutations in RGR, encoding a light-sensitive opsin homologue, in patients with retinitis pigmentosa. *Nat Genet.* 1999;23:393-394.
9. Arno G, Hull S, Carss K, et al. Reevaluation of the retinal dystrophy due to recessive alleles of RGR with the discovery

- of a cis-acting mutation in CDHR1. *Invest Ophthalmol Vis Sci*. 2016;57:4806–4813.
10. McCulloch DL, Marmor MF, Brigell MG, et al. ISCEV Standard for full-field clinical electroretinography (2015 update). *Doc Ophthalmol*. 2015;130:1–12.
 11. Bach M, Brigell MG, Hawlina M, et al. ISCEV standard for clinical pattern electroretinography (PERG): 2012 update. *Doc Ophthalmol*. 2013;126:1–7.
 12. Marmor MF, Brigell MG, McCulloch DL, et al. ISCEV standard for clinical electroretinography (2010 update). *Doc Ophthalmol*. 2011;122:1–7.
 13. Hull S, Mukherjee R, Holder GE, et al. The clinical features of retinal disease due to a dominant mutation in RPE65. *Mol Vis*. 2016;22:626–635.
 14. Sun LW, Johnson RD, Williams V, et al. Multimodal imaging of photoreceptor structure in choroideremia. *PLoS One*. 2016; 11:e0167526.
 15. Michaelides M, Holder GE, Bradshaw K, et al. Cone-rod dystrophy, intrafamilial variability, and incomplete penetrance associated with the R172W mutation in the peripherin/RDS gene. *Ophthalmology*. 2005;112:1592–1598.
 16. Audo I, Friedrich A, Mohand-Saïd S, et al. An unusual retinal phenotype associated with a novel mutation in RHO. *Arch Ophthalmol*. 2010;128:1036–1045.
 17. Wang JS, Kefalov VJ. The cone-specific visual cycle. *Prog Retin Eye Res*. 2011;30:115–128.
 18. Bowne SJ, Humphries MM, Sullivan LS, et al. A dominant mutation in RPE65 identified by whole-exome sequencing causes retinitis pigmentosa with choroidal involvement. *Eur J Hum Genet*. 2011;19:1074–1081.
 19. Arno G, Agrawal SA, Eblimit A, et al. Mutations in REEP6 cause autosomal-recessive retinitis pigmentosa. *Am J Hum Genet*. 2016;99:1305–1315.
 20. Khan KN, El-Asrag ME, Ku CA, et al. Specific alleles of CLN7/MFSD8, a protein that localizes to photoreceptor synaptic terminals, cause a spectrum of nonsyndromic retinal dystrophy. *Invest Ophthalmol Vis Sci*. 2017;58:2906–2914.